Bioelectrochemistry 136 (2020) 107591

Contents lists available at ScienceDirect

Bioelectrochemistry

journal homepage: www.elsevier.com/locate/bioelechem

A photoelectrochemical biosensor for rapid and ultrasensitive norovirus detection

Jiubiao Guo [a,b,§], Dan Liu [c,§], Zhiqiang Yang [d], Wenchuan Weng [e], Edward Wai Chi Chan [d], Zhenling Zeng [b], Kwok-Yin Wong [d], Peng Lin [f,*], Sheng Chen [d,g,*]

[a] Guangdong Key Laboratory of Regional Immunity and Diseases, Department of Pathogen Biology, Shenzhen University School of Medicine, Shenzhen, China
[b] Guangdong Provincial Key Laboratory of Veterinary Pharmaceutics Development and Safety Evaluation, College of Veterinary Medicine, South China Agricultural University, Guangzhou, China
[c] Key Laboratory of Optoelectronic Devices and Systems of Ministry of Education and Guangdong Province, College of Physics and Optoelectronic Engineering, Shenzhen University, Shenzhen 518060, China
[d] Shenzhen Key Laboratory for Food Biological Safety Control, Food Safety and Technology Research Centre, The Hong Kong PolyU Shenzhen Research Institute, Shenzhen, China
[e] Department of Supervision on Import & Export Food Safety, Guangdong Entry-Exit Inspection and Quarantine Bureau, Guangzhou, Guangdong, China
[f] Shenzhen Key Laboratory of Special Functional Materials & Guangdong Research Center for Interfacial Engineering of Functional Materials, College of Materials Science and Engineering, Shenzhen University, Shenzhen 518060, China
[g] Department of Infectious Diseases and Public Health, Jockey Club College of Veterinary Medicine and Life Sciences, City University of Hong Kong, Kowloon, Hong Kong

ARTICLE INFO

Article history:
Received 1 February 2020
Received in revised form 26 June 2020
Accepted 26 June 2020
Available online 1 July 2020

Keywords:
Photoelectrochemical biosensor
Norovirus
VP1
Monoclonal antibody
QD

ABSTRACT

The highly contagious norovirus (NoV) is the most common causative agent of acute gastroenteritis, resulting in >200,000 deaths worldwide annually. A rapid and sensitive detection method is a prerequisite for effective prevention and timely identification of NoV contamination. In the present study, we developed a photoelectrochemical (PEC) biosensor coupled with a novel custom-made monoclonal antibody (mAb) for specific and sensitive NoV detection. Our system could detect levels of recombinant NoV capsid protein VP1 as low as 2×10^{-10} g mL^{-1} (4.9 pM) within 30 min in a concentration-dependent manner. More importantly, the biosensor was versatile in detecting virus isolated from real samples that were as low as 46 copies μL^{-1}. These findings indicate that this system has the potential to serve as a convenient point-of-care system for diagnosing NoV infection and detecting NoV-contaminated food samples.

1. Introduction

Norovirus (NoV) is the most common cause of acute gastroenteritis in humans. This contagious virus was the first viral agent linked to gastrointestinal disease [1]. NoV infection is responsible for ~90% of the epidemic, nonbacterial outbreaks of severe gastroenteritis worldwide [2–4]. Due to the extreme culture requirements, it was not possible to achieve human NoV replication *in vitro* until a method reported by Ettayebi K. and colleagues became available in 2016. This culture method promoted the research and development of effective drugs and vaccines against NoV [3,5].

NoV is a single-stranded, non-enveloped, positive-sense RNA virus. Genetically, NoV can be classified into 10 genogroups (GI-GX) and at least 49 genetic clusters or genotypes [6]. Molecular epidemiology studies recently demonstrated that the variant genotype GII.4 is responsible for ~70% of NoV-related outbreaks [7–9]. The ~7.5 kb NoV genome is organized into three main open read frames (ORF) that encode different viral proteins during the NoV life cycle [1]. In ORF1, a preserved Pol region is often regarded as a primer target site for the identification of NoV genogroups and genotypes through RT-PCR [10]. On the other hand, electron microscopy is a classic diagnostic method for detecting NoV or other small, round-structured viruses with a diameter of 27–30 nm, but it is impracticable for clinical use due to the requirement for high-level technical input and expensive equipment [11]. The immuno-enzymatic method is another alternative for detecting NoV; here, NoV capsid proteins are regarded as binding targets for virus antigen recognition [12]. However, commercial detection kits tend to offer low diagnostic sensitivity, probably due to the

* Corresponding authors at: Department of Infectious Diseases and Public Health, Jockey Club College of Veterinary Medicine and Life Sciences, City University of Hong Kong, Kowloon, Hong Kong, China
E-mail addresses: lin.peng@szu.edu.cn (P. Lin), shechen@cityu.edu.hk (S. Chen).
§ These authors contributed equally to this work.

https://doi.org/10.1016/j.bioelechem.2020.107591
1567-5394/

low binding affinity of the commercially available antibody [13,14].

To overcome the technical limitations and to develop promising alternative techniques for ready-to-use and sensitive NoV detection, biosensors coupled with a range of NoV-specific agents have been developed. Affinity peptide-guided electrochemical biosensors have been recently developed that can sensitively detect NoV with a detection limit of 7.8 copies mL^{-1} human NoV, 99.8 nM recombinant noroviral capsid protein (rP2) [15], or 1.78 gc mL^{-1} HuNoV GII.4 and 2.47 gc mL^{-1} NoV for oysters [16]. In addition, a GII antibody has been coupled with localized surface plasmon resonance or colorimetric bioassays for sensitive and specific NoV detection [17,18]. However, further improvement is needed in the sensitivity and convenience of these newly developed detection approaches.

The discovery of the semiconductor quantum dot (QD) has opened a new nanotechnology age, and its use in electronics and catalysis fields has surged, proving to be an excellent choice for luminescent probes in NoV detection and various other applications [19–21]. A photoelectrochemical (PEC) biosensor is an advanced version of the traditional electrochemically based detection technology; it has the advantages of being inexpensive, simple-to-use, sensitive and having a low noise signal. By using light as the excitation source, PEC biosensors can be designed to potentiometrically or amperometrically detect signal transduction on the surface of inorganic, organic or hybrid semiconductor photoactive materials [22,23]. In addition, compared with other electrochemical transducers, indium tin oxide (ITO) electrodes—which have low surface resistivity and are chemically stable, feasible for biochemical modification and inexpensive—are usually applied in PEC-based biosensor development [24].

The combination of QDs with PEC immunoassays has gained substantial attention, and now constitutes a new branch of bioanalysis [25]. In brief, the principle of a QD-coupled PEC system is that before modification of the platform and upon activation by external energy ($h\nu$), electrons (e^-) (in the form of a photocurrent) can be smoothly transferred from the valence band (VB, lower energy band) to the conduction band (CB, higher energy band). After modification, the photocurrent would be decreased by the steric hindrance arising from immobilized reactants [26]. PEC and QD-based biosensors have been integrated into immunoassays for the cardiac marker troponin T (cTnT) [27], and for pcDNA3-HBV detection [28]. Moreover, a CdSe–ZnO-based photoelectrochemical biosensor was developed to detect NoV RNA with a detection limit of 0.50 nM [29].

In the present study, we aimed to further improve on PEC-based NoV detection. We combined a PEC and QD-based biosensor with our novel custom-made monoclonal antibody specific to the capsid protein VP1 of NoV. The developed sensitive PEC-based biosensor platform enabled us to develop a specific, rapid and sensitive method for NoV detection.

2. Materials and methods

2.1. Materials

ITO glass (ITO coating 180 ± 20 nm, 8.1 ± 0.6 Ω cm^{-2}) was purchased from Southern Glass Holding Co. LTD (Shenzhen, China). $CdCl_2{\cdot}2.5H_2O$ was purchased from Jinshan Tingxin Chemical Plant (Shanghai, China); $Na_2S{\cdot}9H_2O$ was purchased from Lingfeng Chemical Reagent Co. LTD (Shanghai, China); 20 wt% Poly (diallyldimethylammonium chloride) (PDDA) solution, 1-Ethyl-3-(3-dimethylaminopropyl) carbodiimide (EDC) and bovine serum albumin (BSA) were purchased from Sigma-Aldrich (St. Louis, MO, USA); and N-Hydroxysuccinimide (NHS), ascorbic acid (AA), thioglycolic acid (TGA) and monoethanolamine (MEA) were purchased from Sinopharm Chemical Reagent Co., Ltd. (Shanghai, China). Phosphate-buffered saline (PBS) and all other reagents or buffers were prepared using water from an ultra-pure Milli-Q Water System. Virus samples were isolated and concentrated from patients with permission, inactivated at 98 °C for 20 min, diluted with 0.1 M PBS and stored at −80 °C. ELISA Accessory Packs were purchased from Abcam (UK).

2.2. Preparation of mAb specifically targeting VP1 of NoV

A 37 aa peptide (VQAPNGEFTVSPRNSPGEVLLNLELGPELNPYLAHLC) from the NoV GII.12 capsid protein VP1 (YP_009237898.1) was synthesized and used as an antigen to prepare the mAb by Beijing Protein Innovation (Beijing, China). Ascites were produced by injecting hybridoma cells (5×10^5-9×10^5 cells mL^{-1}) that specifically produced anti-VP1-mAb in the peritoneal cavities of paraffin oil-pretreated BALB/c mice. The mAb generated was purified using the Protein G Sepharose 4 Fast Flow System (GE Healthcare, Sweden) and analyzed by SDS-PAGE with BSA as the standard. All animal experiments were performed according to a protocol approved by the Research Animal Care and Use Committee of Hong Kong Polytechnic University. Purified antibodies were stored in 0.1 M PBS and −80 °C for future use.

2.3. Preparation of CdS QDs and ITO electrodes

TGA-stabilized CdS QDs were synthesized as previously described, with modifications [27]. In brief, 250 μL TGA was mixed with 50 mL 0.01 M $CdCl_2$ solution in the presence of N_2 for 30 min; the pH of the mixture was adjusted to 11 with freshly prepared 1.0 M NaOH. Then, 5.5 mL 0.1 M Na_2S was injected and refluxed under N_2 for 4 h. The TGA-stabilized CdS QDs were diluted with deionized (DI) water and stored at 4 °C. ITO electrodes with a working area of 0.25 cm^2 were soaked in 0.6 mL 2% PDDA (0.5 M NaCl solution) for 10 min, followed by another four rounds in 0.6 mL CdS solution for a further 10 min. The fabricated ITO electrodes (ITO/CdS) were stabilized at RT overnight in a dark environment. The ITO electrodes were activated in 1 mL EDC/NHS (20 mg mL^{-1}/10 mg mL^{-1}) at RT for 1 h and washed with DI water three times. The activated ITO electrodes were treated with 25 μL mAb for another 1 h at RT followed by washing three times in 0.01 M PBS. The mAb-conjugated ITO/CdS electrodes (ITO/CdS/mAb) were further treated with 25 μL of VP1 protein at different concentrations at 37 °C for the indicated time and washed in 0.01 M PBS to produce the ITO/CdS/mAb/VP1 electrodes. To test the inactivated virus samples, the VP1 protein was replaced by different concentrations of a virus sample solution in preparation of the ITO/CdS/mAb/NoV electrodes.

2.4. Electrode characterization

An electrochemical impedance spectroscopy (EIS) analysis of the electrodes was performed using a VMP-300 instrument (Bio-Logic Science Instruments, France). In brief, a fabricated ITO electrode as the working electrode, a Pt wire as the counter electrode and a saturated Ag/AgCl electrode as the reference electrode were partially soaked in an assay buffer comprising 5.0 mM $K_3Fe(CN)_6$/$K_4Fe(CN)_6$ (1:1), 0.1 M KCl. The electrodes were connected to a VMP-300 in the single sine mode; the parameters were set with E ranging from −10 to 10 V, Va as 5.0 mV, pw as 0.1, the bandwidth as 8, fi as 100 kHz, and ff as 100 mHz.

2.5. PEC for VP1 or NoV detection

The gene encoding the NoV GII.12 capsid protein VP1 (1-350aa, YP_009237898.1) was synthesized by Tech Dragon Ltd. (Hong Kong, China), subcloned into a pET-15b expression vector, and expressed and purified from the *Escherichia coli* system (BL21, DE3). Viruses from real samples were prepared by GDCIQ (Guangdong Entry-Exit Inspection and Quarantine Bureau) and quantified by RT-qPCR. Based on the specific interaction between the mAb, the recombinant VP1 and the inactivated NoV via the natural VP1 on the surface of NoV, the corresponding changes in current were monitored. In this study, the PEC measurement was conducted by a homemade system connected to an irradiation source of a 500 W Xe lamp (LSH-X500) coupled to a monochromator. The photocurrent was measured using an electrochemical workstation (CHI660E, China). The assay electrolyte of 0.1 M PBS containing 0.1 M ascorbic acid was freshly prepared. All measurements were performed at least three times to ensure consistency.

2.6. VP1 or NoV detection by conventional ELISA

The recombinant VP1 or inactivated-NoV was detected by conventional ELISA method. The experimental procedure was performed by following the instructions of the supplier (abcam, USA). In brief, a high-binding 96-well microplate was first incubated with serially diluted VP1 or NoV for 2 h at RT and rinsed with 1X Wash Buffer three times; next, the microplate was blocked with 1X Blocking Buffer to reduce nonspecific binding for 2 h at RT. Then, 50 μL mAb (2 μg mL^{-1}) was added, and the microplate was incubated for a further 2 h at RT. After rinsing three times, an HRP-labeled anti-mouse IgG (Abcam, UK) was added, and the microplate was incubated for 1 h at RT, followed by TMB substrate incubation for 20 min in the dark. Finally, a solution was added to stop the reactions. The absorbance at 450 nm was measured using a microplate reader (Epoch 2, Bio Tek, USA).

3. Results and discussion

3.1. Principle of PEC biosensor

In the present study, we conjugated isopropanol-pretreated ITO electrodes with PDDA/CdS via electrostatic interactions in the present NoV detection system to form successive layers on the surface of the ITO electrode. We then immobilized the custom-made NoV capsid protein VP1-specific mAb onto CdS QDs with the help of EDC/NHS. By this approach, the VP1 protein, if present, would be captured by the mAb (Schematic 1A). The detection mechanism of the PEC biosensor is based on detecting the steric hindrance changes due to the specific recognition of the conjugated mAb by the VP1 protein of NoV (Schematic 1B). Prior to modification, the CdS QDs could be activated by external energy ($h\upsilon$), resulting in electrons moving from VB to CB, forming electron-hole pairs. Electrons in the CB of the CdS QDs would be further transferred to the band of ITO electrodes in the form of a photocurrent. Meanwhile, the concomitant hole in the VB of CdS QDs would be neutralized by electron donors in the electrolyte (AA solution in the present case). Effective coupling of the procedures at each stage was necessary for continuous photocurrent generation (Schematic 1B upper panel). Upon modification, the insulating features of the proteins and steric hindrance introduced would interfere with or prevent electron-hole neutralization and decrease or diminish photocurrent generation (Schematic 1B lower panel) [26].

3.2. PEC biosensor for recombinant VP1 detection

The VP1 encoded by the second ORF in the NoV genome is a structural protein involved in the formation of the NoV icosahedral capsid [1,30]. In this study, we purified the VP1 protein as a recombinant protein; the corresponding mAb was prepared as described previously and then immobilized onto the surface of ITO/CdS electrodes via EDC/NHS.

To investigate an appropriate concentration ratio between the mAb and the recombinant VP1 protein, we modified activated ITO/CdS electrodes by various concentrations of mAb (0.2, 1 and 5 mg mL^{-1}), followed by incubation with different concentrations of VP1 (0.2 and 2 mg mL^{-1}) at 37 °C for 30 min. Unexpectedly, 5 mg mL^{-1} mAb could not further improve the photocurrent change when compared with that of 1 mg mL^{-1} mAb (Fig. 1A). This finding lead to the questions as to whether the photocurrent change is time-dependent. We thus tested the effects of incubation time on photocurrent change. Our data indicated that the photocurrent change positively correlated with incubation time in the first 30 min, but an incubation time >30 min could not further enhance the photocurrent change (Fig. 1B). A possible explanation for this phenomenom is that the limited working area (0.25 cm^2) in the ITO/CdS electrode could be saturated by 1 mg mL^{-1} mAb and could be recognized and saturated by 0.2 mg mL^{-1} VP1 recombinant protein in 30 min incubation.

Based on our optimization data, we conclude that the optimal concentration for the present sensor was 1 mg mL^{-1} mAb. This concentration was sufficient to saturate the electrode, which would be further saturated by 0.2 mg mL^{-1} VP1 recombinant protein in 30 min.

3.3. EIS analysis of the fabricated ITO electrodes

In principle, impedance is simply the opposition force to electrical current, and the impedance spectrum is often analyzed in an equivalent circuit [31,32]. The EIS method is a powerful tool for investigating the mechanisms of electrochemical research, in which a small-amplitude voltage perturbation is introduced and the impedance Z at different frequencies of the corresponding system is determined (Fig. 2A). A Nyquist plot, which plots the real part impedance Z' and the imaginary part impedance -Z″, is one way to illustrate an impedance measurement [33]. Recently, an increasing number of label-free detection tools for biosensors based on selective interaction between the electrode and target analytes have been developed by harnessing the EIS technique [34].

To verify the modifications of the ITO electrodes at each stage, we used EIS technology for electrode characterization. As expected, the ITO/CdS electrode displayed the lowest impedance in the form of the smallest semicircle diameter; after mAb (1 mg mL^{-1}) or VP1 (2×10^{-4} g mL^{-1}) modification, the impedance of the corresponding electrodes increased due to the surface blocking by nonconductive proteins (Fig. 2B). Overall, the results of our EIS analysis indicated that the ITO electrodes were successfully modified, causing a change in the steric hindrance on the surface of electrodes that was detectable in the form of photocurrent attenuation.

3.4. Sensitivity and specificity analysis of PEC biosensor for GII NoV detection

The sensitivity of the PEC biosensor was determined using various concentrations of VP1 protein (ranging from 2×10^{-4} to 2×10^{-10} g mL^{-1}). Here, we found that the electrode photocurrent changed according to the variation in the concentrations of VP1 protein (Fig. 3). For clarity, the following equation would be applied to determine the photocurrent change ratio.

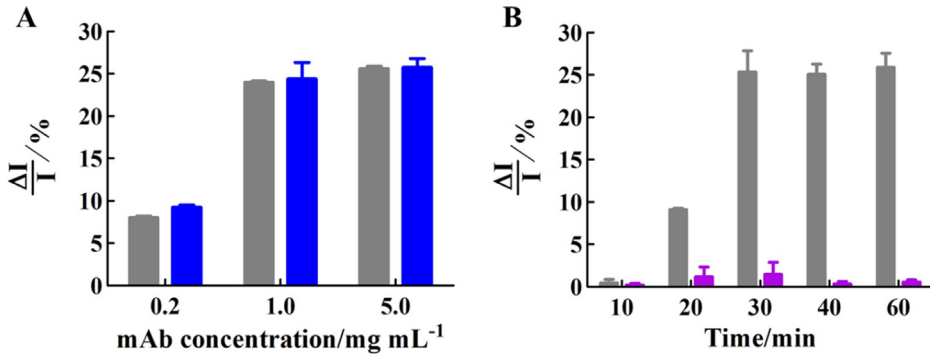

Fig. 1. Optimization of the mAb concentration (A) and incubation time (B). The equation in calculating ΔI/I is illustrated in the following text. At least three tests were performed. Grey column: 0.2 mg mL^{-1} VP1; Blue column: 2 mg mL^{-1} VP1; Purple column: 0.1 M PBS.

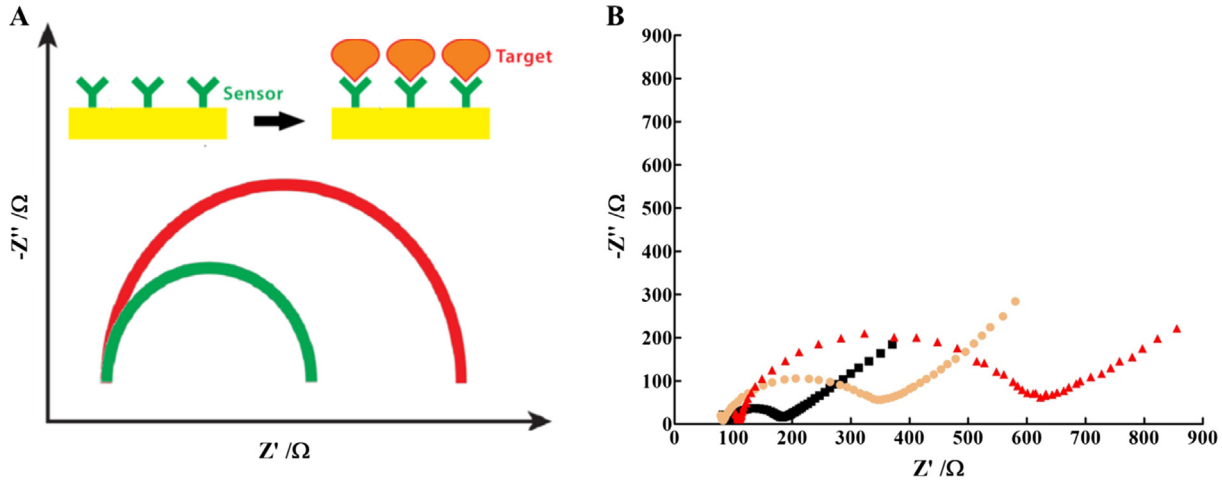

Fig. 2. The principle of EIS and electrode characterization. (A) A general scheme for label-free detection biosensor and electrode characterization using the EIS technique. This image has been redrawn with modifications from Chang and Park 2010. (B) A Nyquist plot to characterize successfully modified electrodes. The EIS analysis experiments were repeated at least three times for constant results using a VMP-300 instrument. The mAb concentration was 1 mg mL^{-1}, and VP1 was 2×10^{-4} g mL^{-1}. Abbreviations: Z', real part impedance; -Z″, imaginary part impedance. Black squares: ITO/CdS; Orange circles: ITO/CdS/mAb; Red triangle: ITO/CdS/mAb/VP1.

$$\frac{\Delta I}{I} = \frac{(I^0_{max} - I^0_{min}) - (I^i_{max} - I^i_{min})}{I^0_{max} - I^0_{min}} \quad (1)$$

Where I^0_{max} and I^0_{min} represents the maximum (light on) and minimum (light off) photocurrents of the ITO/CdS/mAb electrode, respectively. After incubation with different concentrations of VP1, I^i_{max} and I^i_{min}, representing the maximum and minimum photocurrents of the corresponding ITO/CdS/mAb/VP1 electrode, respectively, were measured.

On average, a 24% photocurrent change ratio was determined in the present of 2×10^{-4} g mL^{-1} VP1 protein (Fig. 3A, D); the ratios for 2×10^{-6} g mL^{-1} and 2×10^{-10} g mL^{-1} VP1 were ~13% and ~5%, respectively (Fig. 3B–D). The molecular weight of the recombinant VP1 protein was ~41,000 g mol^{-1} (371 residues including His tag). Thus, the limit of detection (LOD) of the biosensor was 4.9 pM (the lowest concentration of VP1 protein divided by the molar of VP1 protein, or 2×10^{-10} g mL^{-1}/41,000 g mol^{-1}). This LOD was ~2×10^4-fold higher in sensitivity than that of an affinity peptide-based electrochemical biosensor in NoV detection (99.8 nM) [15] and 20-fold higher than that of a graphene-gold nanocomposite aptasensor (100 pM) [35]. Taken together, our PEC biosensor could rapidly and ultra-sensitively detect levels as low as 2×10^{-10} g mL^{-1}, or 4.9 pM NoV VP1 protein in 30 min incubation.

Next, we analyzed the specificity of the developed PEC biosensor for detecting the NoV capsid protein VP1. We used PBS, BSA and SNAP25 (soluble NSF attachment protein of 25 kDa) [36] as the controls. We found that 0.1 M PBS, 2 mg mL^{-1} BSA or 4 mg mL^{-1} SNAP25 exerted negligible effects on the photocurrent (Fig. 4A). However, we detected an ~24% photocurrent change ratio with 2×10^{-4} g mL^{-1} VP1, indicating a high specificity of the biosensor towards the VP1 protein. Then we checked the feasibility of the PEC biosensor in detecting NoV particles using different NoV genotypes and rotavirus A. We determined the virus concentrations by RT-qPCR (data not shown). As expected, the PEC sensor could specifically detect different NoV genotypes with similar detection efficiencies, but it could not detect rotavirus A. These data support the specificity of the developed PEC towards NoV (Fig. 4B).

Next, we serially diluted samples of the NoV GII.12 genotype to test the sensitivity of the PEC sensor. Here we found an ~35% photocurrent change ratio could be detected from 4688 copies μL^{-1} NoV GII.12; 468 copies μL^{-1} NoV gave rise to a slightly higher photocurrent change ratio than that of 2×10^{-4} g mL^{-1} VP1 protein. Furthermore, the 10-fold diluted NoV sample (46 copies μL^{-1}) also caused an ~18% change in photocurrent (Fig. 4B). These data suggest that the PEC biosensor can feasibly and specifically detect NoV particles in a concentration-dependent manner.

We next compared the sensitivity of conventional ELISA technology in detecting VP1 or NoV with that of the developed PEC biosensor. We found that the conventional ELISA method could

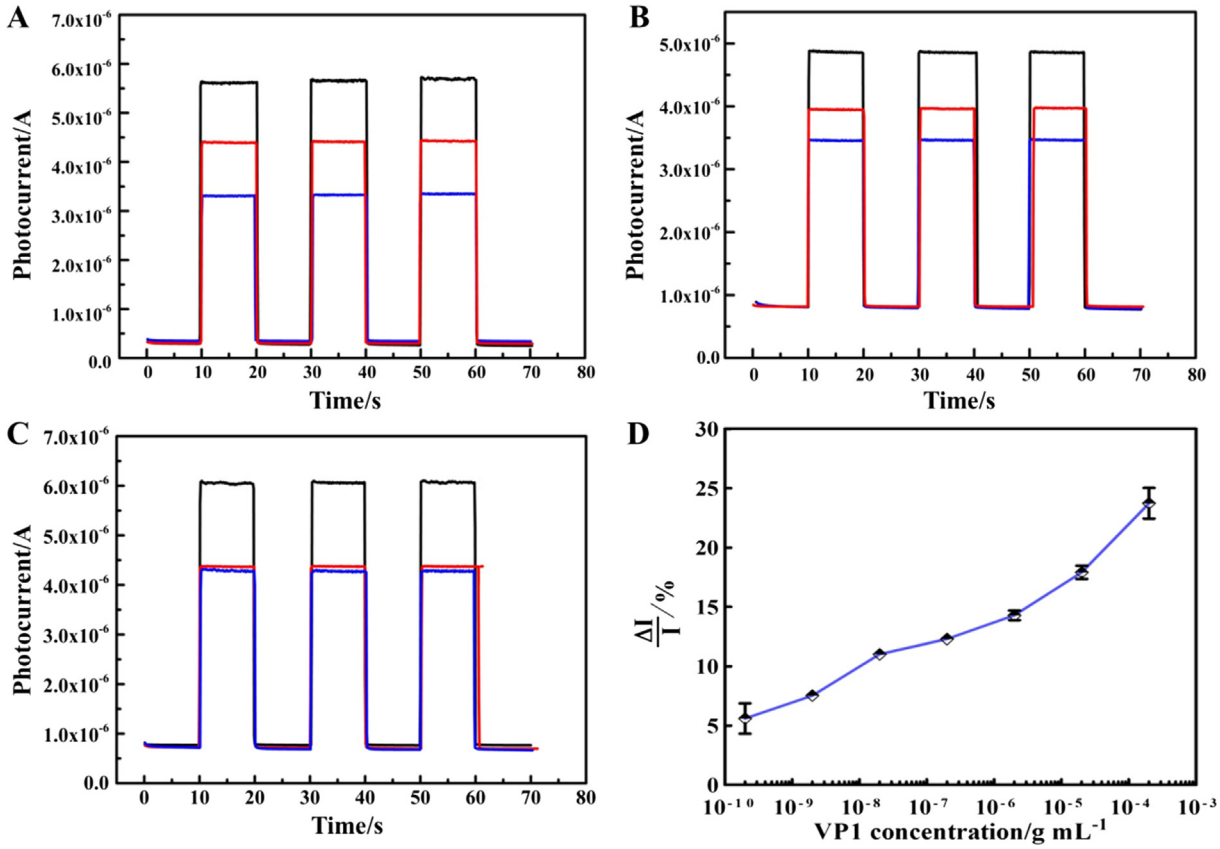

Fig. 3. Detection of the recombinant VP1 NoV protein by the developed PEC biosensor. (A)-(C) illustrate the concentration-dependent change in the photocurrent of electrodes corresponding to (A) 2×10^{-4}, (B) 2×10^{-6} and (C) 2×10^{-10} g mL^{-1} VP1 protein. Black curve: photocurrent trend of ITO/CdS; Red curve: photocurrent trend of ITO/CdS/mAb; Blue curve: photocurrent trend of ITO/CdS/mAb/VP1. (D) The positive correlation between the VP1 concentration and the photocurrent change ratio after 30 min incubation at 37 °C.

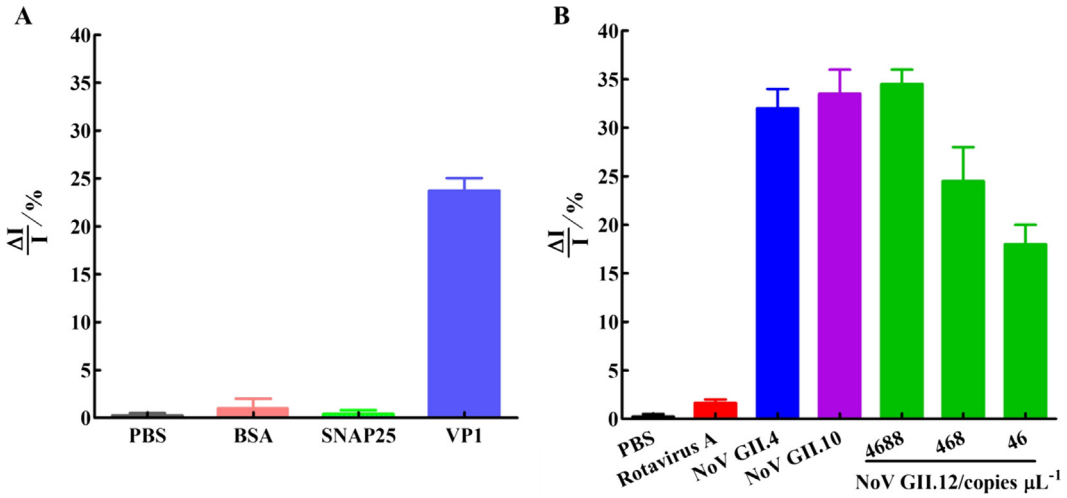

Fig. 4. Specificity and feasibility analysis of the PEC biosensor in detecting recombinant VP1 protein (A) and inactivated virus samples (B). The concentration of BSA, SNAP25 and VP1 was 2 mg mL^{-1}, 4 mg mL^{-1} and 0.2 mg mL^{-1}, respectively, and the concentration of rotavirus A, NoV GII.4 and NoV GII.10 was 5000 copies μL^{-1}. At least three tests were performed to ensure consistency.

detect recombinant VP1 levels as low as 2×10^{-8} g mL^{-1} (Fig. 5A, B upper panel), with ~100-fold lower sensitivity than the PEC biosensor. Interestingly, the conventional ELISA method displayed a similar level of sensitivity in detecting NoV GII.12 compared with the biosensor (Fig. 5A, B lower panel). We thus conclude that our developed PEC biosensor might serve as a promising alternative for detecting NoV with the advantages of high sensitivity and speed, low cost and capacity for point-of-care diagnosis.

We finally searched the available literature for other NoV detection approaches other than ELISA, to see how our new system comapres (Table 1). Takemura *et al.* used GII antibody-guided localized surface plasmon resonance-amplified magnetofluoroim-

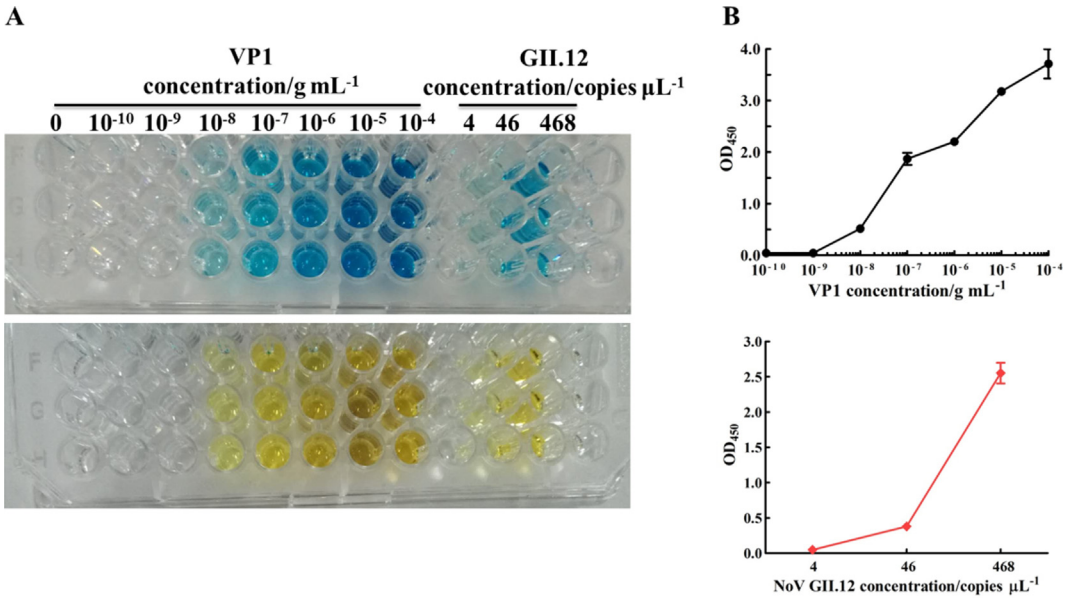

Fig. 5. VP1 and NoV GII.12 detection by conventional ELISA. (A) Color visual detection of VP1 and inactivated NoV at serially diluted concentrations. The upper and lower panels indicate the color visualization before and after the stop solution was added, respectively. (B) Quantitative analysis of VP1 (upper panel) and NoV GII.12 (lower panel) detection by conventional ELISA.

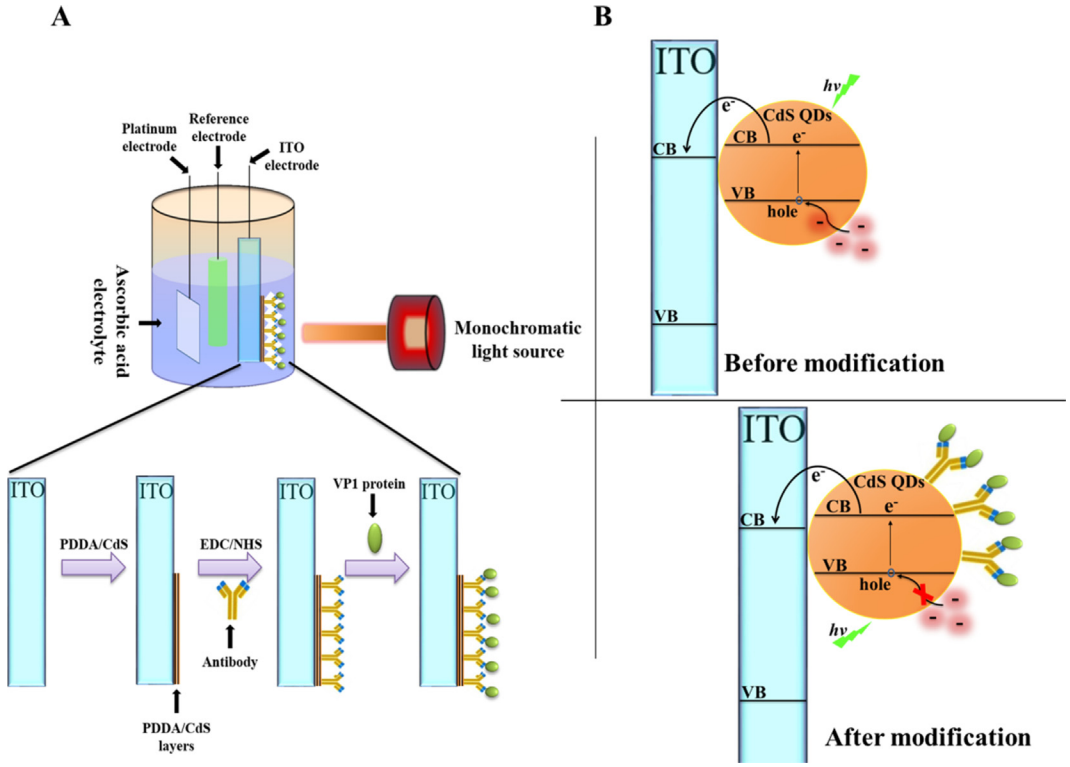

Schematic 1. The design and mechanism of the PEC biosensor for NoV detection. (A) Isopropanol-treated (2 M KOH included) and dried ITO electrodes were alternatively soaked in PDDA and CdS solutions for three cycles, followed by activation by EDC/NHS. An antibody was then conjugated onto the ITO/CdS electrodes. Finally, the VP1 or virus-treated electrodes would be measured under a monochromatic light for the change in photocurrent. (B) Before modification of the platform and upon activation by external energy ($h\nu$), electrons (e^-) in the form of photocurrent could be smoothly transferred from the valence band (VB) to the conduction band (CB) and then to the ITO electrode. After modification, the photocurrent would be decreased by the steric hindrance arising from immobilized antibodies, VP1 or inactivated viruses.

munoassay for NoV detection, and the developed method displayed high specificity toward NoV and a relative high detection limit for NoV VLPs [17]. Meanwhile, Han *et al.* reported that a CdSe–ZnO-based photoelectrochemical biosensor exhibited a disappointing performance in NoV detection [29]. Other technologies, such as aptasensors, immune electron microscopy and RT-PCR,

Table 1
Literature search of NoV detection by various methods.

Detection Method	Linear Range	Detection Limit	Specificity	Reference
GII Ab-guided localized surface plasmon resonance-amplified magnetofluoroimmunoassay	1 pg mL^{-1} to 5 ng mL^{-1} NoV VLPs; $10^2 \sim 10^7$ copies mL^{-1} clinical HuNoV RNA	0.48 pg mL^{-1} NoV VLPs in feces; 84 ~ 934 copies mL^{-1} GII HuNoV	High	[17]
GII Ab-guided colorimetric immunoassay	$10 \sim 10^5$ pg mL^{-1} NoV VLP; $10 \sim 10^4$ (GII.3) and $10^2 \sim 10^5$ (GII.4) copies mL^{-1}	10.8 pg mL^{-1} NoV VLP; 13.2 ~ 16.3 gc mL^{-1} fecal NoV GII.3 and GII.4	High	[18]
Colorimetric NanoZyme aptasensor	200–10,000 viruses mL^{-1}, or 1320–19,800 viruses mL^{-1}, or 3300–33,000 viruses mL^{-1}	200 viruses mL^{-1}	High	[38]
Specific binding peptide guided-impedance electrochemical biosensor	0 to 10^4 copies mL^{-1} HuNoV GII.4; 10 to 10^5 copies mL^{-1}	1.78 gc mL^{-1} HuNoV GII.4 and 2.47 gc mL^{-1} NoV from oysters	High	[16]
CdSe–ZnO-based photoelectrochemical biosensor	0 ~ 5.10 nM NoV RNA	0.50 nM	N/A	[29]
Molecular beacon-AuNR@CdSeTe-based biosensor	2 ~ 18 copies mL^{-1}	1.2 copies mL^{-1}	High	[39]
Surface plasmon resonance-assisted fluoroimmunosensor	0.01 ~ 1 ng mL^{-1}	0.01 ng mL^{-1}	N/A	[19]
Surface-enhanced Raman scattering-based immunoassay	$1.0 \times 10^6 \sim 2.5 \times 10^8$ viruses mL^{-1}	1×10^6 viruses mL^{-1}	N/A	[40]
Anti-VP1 antibody guided photoelectrochemical biosensor	2×10^{-4} to 2×10^{-10} g mL^{-1}	2×10^{-10} g mL^{-1} (4.9 pM) VP1; 46 copies μL^{-1} GII.12	High	This work

have been described for detecting NoV, but the data indicate that the immune-coupled biosensor elicits the most satisfactory performance, even for real sample detection [18,37].

4. Conclusions

Based on their specific antigen-antibody recognition and photoelectric effects, newly developed PEC immunoassays have attracted great attention. Here, we designed and prepared a novel monoclonal antibody that specifically recognizes norovirus VP1, and inactivated NoV virus. By combining the novel antibody with CdS QDs and ITO electrodes, we successfully developed a new PEC biosensor that enables rapid and ultrasensitive NoV detection. After just 30 min treatment, our system can specifically detect NoV VP1 protein levels as low as 2×10^{-10} g mL^{-1} or 4.9 pM. More importantly, our biosensor is versatile in specifically detecting different norovirus genotypes, suggesting that our detection system has the potential to serve as an alternative, ready-to-use and point-of-care tool for clinical diagnosis in the future.

Author contributions

Jiubiao Guo designed and conducted the experiments, analyzed the data, and wrote the manuscript. Dan Liu, Zhiqiang Yang and Wenchuan Weng designed, conducted the experiments, and analyzed the data. Edward Wai Chi Chan, Zhenling Zeng and Kwok-Yin Wong designed the experiment and edited the manuscript. Peng Lin and Sheng Chen initiated and supervised the project and edited the manuscript.

Declaration of Competing Interest

There are no conflict of interests to declare.

Acknowledgments

This work was supported by the Basic Research Fund of Shenzhen (20170410160041091), the Guangzhou International Science and Technology Cooperation Program (2014J4500027), the AQSIQ Research Program of China (2015IK252), National Natural Science Foundation of China (31800064) and the Shenzhen Science and Technology Innovation Commission grant (JCYJ20180507182049853, JCYJ20170818104557243). The authors would like to thank Dr. Jessica Tamanini (Shenzhen University Health Science Centre) for proof-reading the manuscript prior to submission.

References

[1] S.G. Morillo, C. Timenetsky Mdo, Norovirus: an overview, Rev. Assoc. Med. Bras. 57 (2011) 453–458.
[2] L. Lindesmith, C. Moe, S. Marionneau, N. Ruvoen, X. Jiang, L. Lindblad, P. Stewart, J. LePendu, R. Baric, Human susceptibility and resistance to Norwalk virus infection, Nat. Med. 9 (2003) 548–553.
[3] N.W. Cortes-Penfield, S. Ramani, M.K. Estes, R.L. Atmar, Prospects and challenges in the development of a norovirus vaccine, Clin. Ther. 39 (2017) 1537–1549.
[4] A.J. Hall, B.A. Lopman, D.C. Payne, M.M. Patel, P.A. Gastanaduy, J. Vinje, U.D. Parashar, Norovirus disease in the United States, Emerg. Infect. Dis. 19 (2013) 1198–1205.
[5] K. Ettayebi, S.E. Crawford, K. Murakami, J.R. Broughman, U. Karandikar, V.R. Tenge, F.H. Neill, S.E. Blutt, X.L. Zeng, L. Qu, B. Kou, A.R. Opekun, D. Burrin, D.Y. Graham, S. Ramani, R.L. Atmar, M.K. Estes, Replication of human noroviruses in stem cell-derived human enteroids, Science 353 (2016) 1387–1393.
[6] P. Chhabra, M. de Graaf, G.I. Parra, M.C. Chan, K. Green, V. Martella, Q. Wang, P. A. White, K. Katayama, H. Vennema, M.P.G. Koopmans, J. Vinje, Updated classification of norovirus genogroups and genotypes, J. General Virol. 100 (2019) 1393–1406.
[7] C.I. Gallimore, J. Green, D. Lewis, A.F. Richards, B.A. Lopman, A.D. Hale, R. Eglin, J.J. Gray, D.W. Brown, Diversity of noroviruses cocirculating in the north of England from, 1998 to 2001, J. Clin. Microbiol. 42 (2004) 1396–1401.
[8] E.T. Tu, T. Nguyen, P. Lee, R.A. Bull, J. Musto, G. Hansman, P.A. White, W.D. Rawlinson, C.J. McIver, Norovirus GII.4 strains and outbreaks, Australia, Emerg. Infect. Dis. 13 (2007) 1128–1130.
[9] L. Jia, Y. Zhang, L. Liu, H. Dong, L. Zhao, Y. Qian, High prevalence of GII norovirus in hospitalized children with acute diarrhea, in Beijing, PLoS ONE 12 (2017), e0179839.
[10] J. Vinje, H. Vennema, L. Maunula, C.H. von Bonsdorff, M. Hoehne, E. Schreier, A. Richards, J. Green, D. Brown, S.S. Beard, S.S. Monroe, E. de Bruin, L. Svensson, M. P. Koopmans, International collaborative study to compare reverse transcriptase PCR assays for detection and genotyping of noroviruses, J. Clin. Microbiol. 41 (2003) 1423–1433.
[11] P.J. Wright, I.C. Gunesekere, J.C. Doultree, J.A. Marshall, Small round-structured (Norwalk-like) viruses and classical human caliciviruses in southeastern Australia, 1980–1996, J. Med. Virol. 55 (1998) 312–320.
[12] R.L. Atmar, M.K. Estes, Diagnosis of noncultivatable gastroenteritis viruses, the human caliciviruses, Clin. Microbiol. Rev. 14 (2001) 15–37.
[13] R.A. Bull, E.T. Tu, C.J. McIver, W.D. Rawlinson, P.A. White, Emergence of a new norovirus genotype II.4 variant associated with global outbreaks of gastroenteritis, J. Clin. Microbiol. 44 (2006) 327–333.
[14] S. Castriciano, K. Luinstra, A. Petrich, M. Smieja, C. Lee, D. Jang, E. Portillo, M. Chernesky, Comparison of the RIDASCREEN norovirus enzyme immunoassay to IDEIA NLV GI/GII by testing stools also assayed by RT-PCR and electron microscopy, J. Virol. Methods 141 (2007) 216–219.
[15] H.J. Hwang, M.Y. Ryu, C.Y. Park, J. Ahn, H.G. Park, C. Choi, S.D. Ha, T.J. Park, J.P. Park, High sensitive and selective electrochemical biosensor: Label-free detection of human norovirus using affinity peptide as molecular binder, Biosens. Bioelectron. 87 (2017) 164–170.
[16] S.H. Baek, M.W. Kim, C.Y. Park, C.S. Choi, S.K. Kailasa, J.P. Park, T.J. Park, Development of a rapid and sensitive electrochemical biosensor for detection of human norovirus via novel specific binding peptides, Biosens. Bioelectron. 123 (2019) 223–229.

[17] K. Takemura, J. Lee, T. Suzuki, T. Hara, F. Abe, E.Y. Park, Ultrasensitive detection of norovirus using a magnetofluoroimmunoassay based on synergic properties of gold/magnetic nanoparticle hybrid nanocomposites and quantum dots, Sensor Actuat. B-Chem. 296 (2019).
[18] I.M. Khoris, K. Takemura, J. Lee, T. Hara, F. Abe, T. Suzuki, E.Y. Park, Enhanced colorimetric detection of norovirus using in-situ growth of Ag shell on Au NPs, Biosens. Bioelectron. 126 (2019) 425–432.
[19] H. Ashiba, Y. Sugiyama, X. Wang, H. Shirato, K. Higo-Moriguchi, K. Taniguchi, Y. Ohki, M. Fujimaki, Detection of norovirus virus-like particles using a surface plasmon resonance-assisted fluoroimmunosensor optimized for quantum dot fluorescent labels, Biosens. Bioelectron. 93 (2017) 260–266.
[20] I. Costas-Mora, V. Romero, I. Lavilla, C. Bendicho, An overview of recent advances in the application of quantum dots as luminescent probes to inorganic-trace analysis, TrAC, Trends Anal. Chem. 57 (2014) 64–72.
[21] R. Gill, M. Zayats, I. Willner, Semiconductor quantum dots for bioanalysis, Angew. Chem. 47 (2008) 7602–7625.
[22] A. Ravalli, D. Voccia, I. Palchetti, G. Marrazza, Electrochemical, Electrochemiluminescence, and Photoelectrochemical Aptamer-Based Nanostructured Sensors for Biomarker Analysis, Biosensors (Basel) 6 (2016).
[23] W.W. Zhao, J.J. Xu, H.Y. Chen, Photoelectrochemical bioanalysis: the state of the art, Chem. Soc. Rev. 44 (2015) 729–741.
[24] M. Shokoueinejad, D.W. Park, Y.H. Jung, S.K. Brodnick, J. Novello, A. Dingle, K.I. Swanson, D.H. Baek, A.J. Suminski, W.B. Lake, Z. Ma, J. Williams, Progress in the field of micro-electrocorticography, Micromachines 10 (2019).
[25] J. Shu, D. Tang, Current advances in quantum-dots-based photoelectrochemical immunoassays, Chem. Asian J. (2017).
[26] W.W. Zhao, J. Wang, J.J. Xu, H.Y. Chen, Energy transfer between CdS quantum dots and Au nanoparticles in photoelectrochemical detection, Chem. Commun. (Camb.) 47 (2011) 10990–10992.
[27] W.W. Zhao, R. Chen, P.P. Dai, X.L. Li, J.J. Xu, H.Y. Chen, A general strategy for photoelectrochemical immunoassay using an enzyme label combined with a CdS quantum dot/TiO(2) nanoparticle composite electrode, Anal. Chem. 86 (2014) 11513–11516.
[28] X. Pang, H. Bian, W. Wang, C. Liu, M.S. Khan, Q. Wang, J. Qi, Q. Wei, B. Du, A biochemical application of N-GQDs and g-C3N4 QDs sensitized TiO2 nanopillars for the quantitative detection of pcDNA3-HBV, Biosens. Bioelectron. 91 (2017) 456–464.
[29] Z. Han, Q. Weng, C. Lin, J. Yi, J. Kang, Development of CdSe(-)ZnO flower-rod core-shell structure based photoelectrochemical biosensor for detection of norovirous RNA, Sensors 18 (2018).
[30] T. Tubiana, Y. Boulard, S. Bressanelli, Dynamics and asymmetry in the dimer of the norovirus major capsid protein, PLoS ONE 12 (2017), e0182056.
[31] E.P. Randviir, C.E. Banks, Electrochemical impedance spectroscopy: an overview of bioanalytical applications, Anal. Methods 5 (2013) 1098–1115.
[32] D.D. Macdonald, Reflections on the history of electrochemical impedance spectroscopy, Electrochim. Acta 51 (2006) 1376–1388.
[33] F. Lisdat, D. Schafer, The use of electrochemical impedance spectroscopy for biosensing, Anal. Bioanal. Chem. 391 (2008) 1555–1567.
[34] B.Y. Chang, S.M. Park, Electrochemical impedance spectroscopy, Annu Rev Anal Chem (Palo Alto Calif) 3 (2010) 207–229.
[35] R. Chand, S. Neethirajan, Microfluidic platform integrated with graphene-gold nano-composite aptasensor for one-step detection of norovirus, Biosens. Bioelectron. 98 (2017) 47–53.
[36] S. Chen, J.T. Barbieri, Unique substrate recognition by botulinum neurotoxins serotypes A and E, J. Biol. Chem. 281 (2006) 10906–10911.
[37] L. Liu, M.D. Moore, A survey of Analytical Techniques for Noroviruses, Foods 9 (2020).
[38] P. Weerathunge, R. Ramanathan, V.A. Torok, K. Hodgson, Y. Xu, R. Goodacre, B. K. Behera, V. Bansal, Ultrasensitive colorimetric detection of murine norovirus using nanozyme aptasensor, Anal. Chem. 91 (2019) 3270–3276.
[39] Z.Z. Han, L. Chen, Q.H. Weng, Y. Zhou, L. Wang, C.Y. Li, J.H. Chen, Silica-coated gold nanorod@CdSeTe ternary quantum dots core/shell structure for fluorescence detection and dual-modal imaging, Sensor Actuat. B-Chem. 258 (2018) 508–516.
[40] J.D. Driskell, K.M. Kwarta, R.J. Lipert, M.D. Porter, J.D. Neill, J.F. Ridpath, Low-level detection of viral pathogens by a surface-enhanced Raman scattering based immunoassay, Anal. Chem. 77 (2005) 6147–6154.